ICE THICKNESS AND SEA DEPTH DERIVED FROM REFLECTION-SEISMIC MEASUREMENTS ON THE CENTRAL PART OF FILCHNER-RONNE ICE SHELF, ANTARCTICA

by

J. Determann, F. Thyssen and H. Engelhardt

(Forschungsstelle für physikalische Glaziologie der Westfälischen Wilhelms-Universität, Corrensstraße 24, D – 4400 Münster, Federal Republic of Germany)

ABSTRACT

In January 1986, reflection-seismic measurements were made in the central part of Filchner—Ronne Ice Shelf, north of Henry and Korff ice rises, by a German oversnow traverse. With the help of a newly developed "ice streamer", two people were able to obtain seismic records nearly every 5 km over a distance of 150 km within 3 d. Processing of digitally recorded seismograms yielded profiles of ice thickness and sea depth. The ice thickness varies from 400 to 500 m and is in good agreement with the thickness of 465 m at a drill hole. The reflection-seismic results are comparable with those obtained from aerogeophysical measurements.

INTRODUCTION

There is some uncertainty about ice thickness over a broad area of Filchner—Ronne Ice Shelf (FRIS) down-stream of Henry Ice Rise, Korff Ice Rise and Doake Ice Rumples. Robin and others (1983) assumed ice thicknesses of less than 200 m in places, on the basis of electromagnetic reflection measurements (EMR or RES). A survey by Thyssen (1985, 1986) of a highly reflecting internal horizon at the margin of the ice shelf near the German Filchner Station, west of Berkner Island, raised questions about the earlier data. It appeared that RES measurements had widely detected an internal horizon and not the ice bottom.

Recent reflection-seismic studies by Herrod and Garrett (1986) failed to detect clear reflection signals from the ice bottom, probably due to a diffuse ice—water interface which was a result of freezing and caused a decrease in the reflection coefficient. As modern electromagnetic techniques are not able to penetrate the ice beneath the internal horizon, we started another test, using seismic methods. In January 1986 further seismic investigations were made at the center of FRIS. Figure 1 shows the reference numbers of a geodetic grid net and the locations where seismic measurements were carried out. An ice streamer proposed by Thyssen and towed by a tracked vehicle yielded a record of seismograms every 5 or 10 km without affecting the fast progress of the traverse group.

The processing of 25 seismograms along a 150 km profile from grid point 240 to grid point 335 has yielded details of the trends of the sea floor and ice bottom. They are supplemented by data derived from reflection seismograms which were recorded in 1984 near Filchner Station.

FIELD WORK

The seismograms were digitally recorded by means of a 12 channel amplifier system (Oyo McSeis 1500) with a dynamic range of 72 dB. The cable had a total length of 234 m and contained 12 gimbal-mounted 4.5 cps geophones spaced 18 m apart, and with a 36 m offset between the first
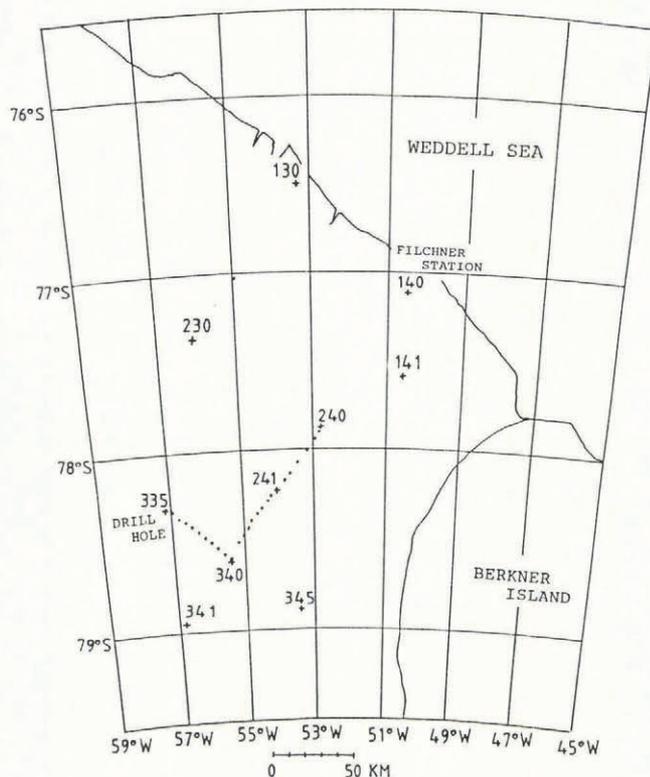

Fig. 1. The central part of Filchner—Ronne Ice Shelf west of Berkner Island. Sites where seismic records were obtained in 1986 are denoted by dots.

geophone and the shot. At every grid point where the traverse group had other glaciological work to do, additional seismograms were recorded with normally planted geophones. These, however, showed no significant improvement.

Because of the limitations of the recording system and after some test shots, the recording-time window was set to 1 s at a sample rate of 1 ms. Explosive charges generally of 1 kg were used in hand-drilled bore holes of approximately 4.5 m depth. With the intention of obtaining multiple reflections from the ice bottom at several shot points, the charge was increased to 4.5 kg while using a delay time up to 500 ms for recording. In at least one case a multiple reflection was detected.

PROCESSING

Every seismic record was processed with standard routines like muting, gain control and filtering. Muting was carried out for at least the first 100 ms of records, in order
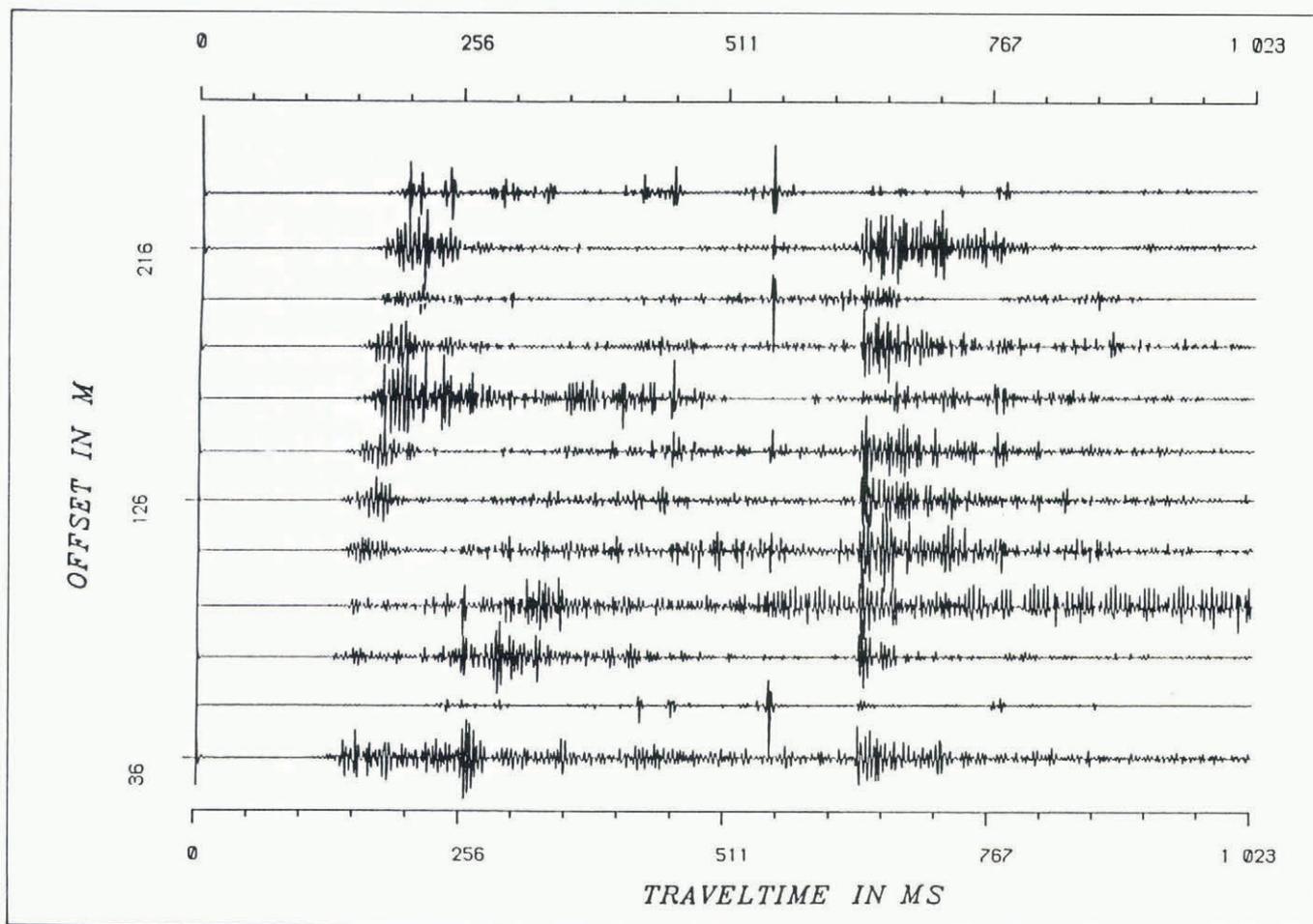
Fig. 2. The processed record from shot point 16 at profile distance 50 km, using 1 kg, ice streamer and filter pass band 80–250 cps. The dominant reflection near $t_0 = 640$ ms must be related to the sea floor, whereas a seismic return from the ice bottom, estimated to lie between 200 and 300 ms, is not visible. The event at 550 ms is electrostatic noise.

to reduce the gain of strong surface waves and refracted waves. Limiting the filter to an optimum pass band from 80 to 250 cps led to further decreases in surface waves and electrostatic noise. Figure 2 shows a typical processed seismogram revealed from the ice streamer at profile km 50 (GP 241). As a result of processing, the signal-to-noise ratio has increased but the record is still electrostatically disturbed (e.g. near 550 ms). Strong reflections, in this case occurring at travel times of about 640 ms, must be related to the return from the sea bottom. Clear evidence of ice-bottom reflections is still not visible.

Rough estimates of the maximum coherency stacking (MCS) velocity of longitudinal waves in the ice and of the known ice thickness of surrounding areas give rise to the assumption that the travel times of the ice–water reflections must be less than about 300 ms. In order to show these returns, data had to be processed more extensively. On the assumption of almost horizontally layered media, without lateral inhomogeneities in the elastic constants, it is permissible to use a simplified form of stacking velocity analysis from a single seismogram (Garotta and Michon 1967).

The modified velocity analysis performs an amplitude stacking of all traces along computed reflection hyperbolas, belonging to different seismic MCS velocities and travel times at shot point t_0. Figure 3 shows the result of this velocity analysis as applied to the processed record in Figure 2, where every trace represents a stacking velocity and expresses the stacked amplitudes depending on t_0. Seismic reflectors are indicated by maxima in amplitude and appear at stacking velocities that give a good approximation of the root mean square (RMS) velocities in the case of horizontal layering. The error in this approximation is minimal when the geophone offset is sufficiently small in comparison with the depth of the seismic reflector, as is the case with the drag cable we used.

As the plot of the velocity analysis contains several maxima, further information is required in order to make a distinction between different horizons. A comparison with the unprocessed seismogram section identifies some of the maxima as arising from electrostatic noise. Furthermore, a knowledge of the MCS velocity enables us to obtain more evidence for seismic returns from the ice bottom. The interpretation of seismic short-refraction lines recorded in 1984 near Filchner Station yielded a velocity–depth profile of approximately the upper 100 m of the ice shelf. From this, an RMS velocity of around 3650 m/s can be computed (for example) for an ice thickness of 400 m, if we assume an ice velocity of 3815 m/s for depths greater than 100 m.

On the realistic assumption that lateral variations in velocity with depth on the inland seismic profile are sufficiently small, we have used a general value of 3650 m/s for the observed area. Taking this RMS velocity, the return from an ice bottom at 500 m depth must appear at travel times of less than 300 ms. A check on the time interval up to $t_0 = 300$ ms and on stacking velocities at a range of 3650 m/s yielded a number of maximum-amplitude events which may be related to an ice-bottom reflection. In order to reduce the number of events which are not real or which have arisen from noise, and to obtain a clearer view of the trend of the ice-bottom reflector, the contents of 24 velocity analyses were combined in one plot. This was done by extracting from each velocity analysis the trace belonging to the chosen RMS velocity and plotting it against profile distance.

The result is shown in Figure 4, and yields further evidence for the existence of an ice-bottom reflector. Obviously the quality of any correlation of reflecting events depends on the distance of shot points. The best correlation is achieved by short-interval measurements where the spacing of shot points is only 5 km, as in the profile section between 50 and 100 km. Over the last five traces
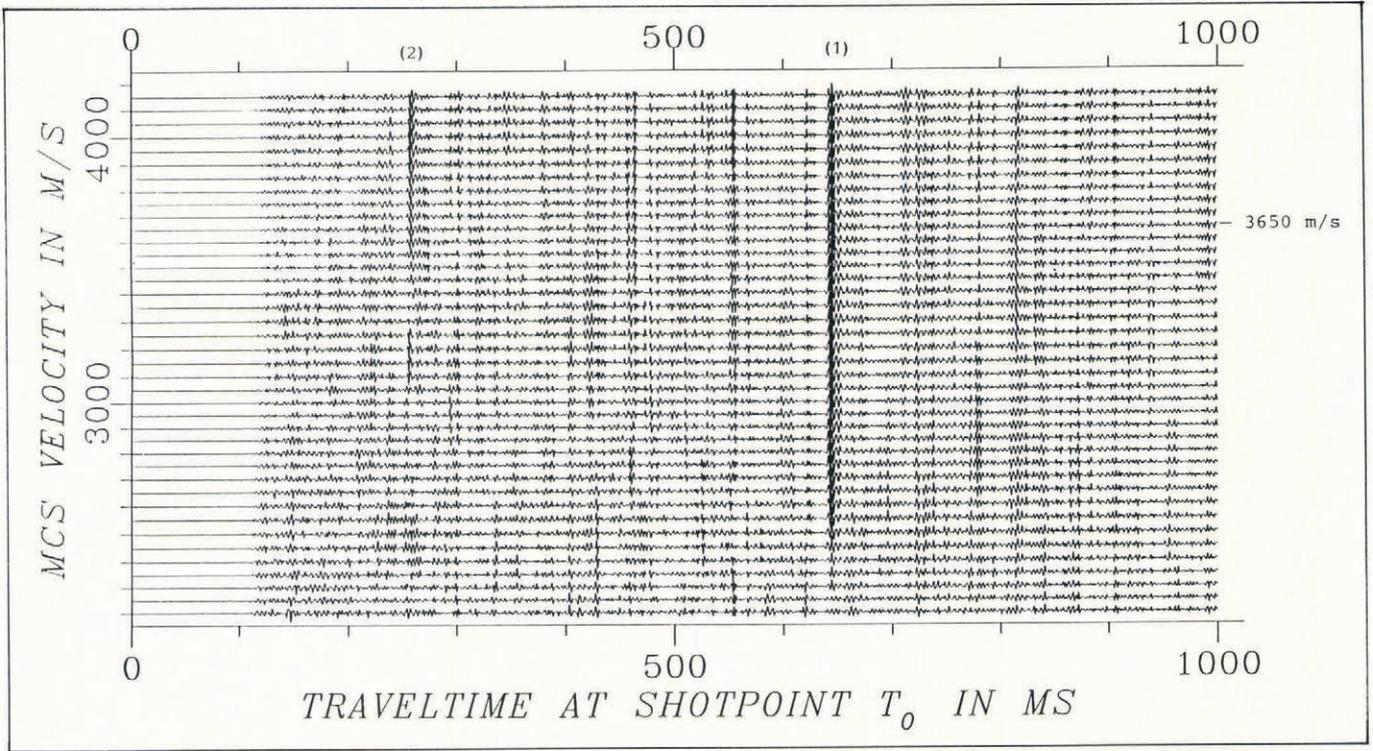
15

Fig. 3. Velocity analysis of the processed seismic record shown in Figure 2. The maximum at $t_0 = 640$ ms (1) corresponds to the reflection from the sea bottom. The assumed ice-bottom reflection is at $t_0 = 270$ ms (2).
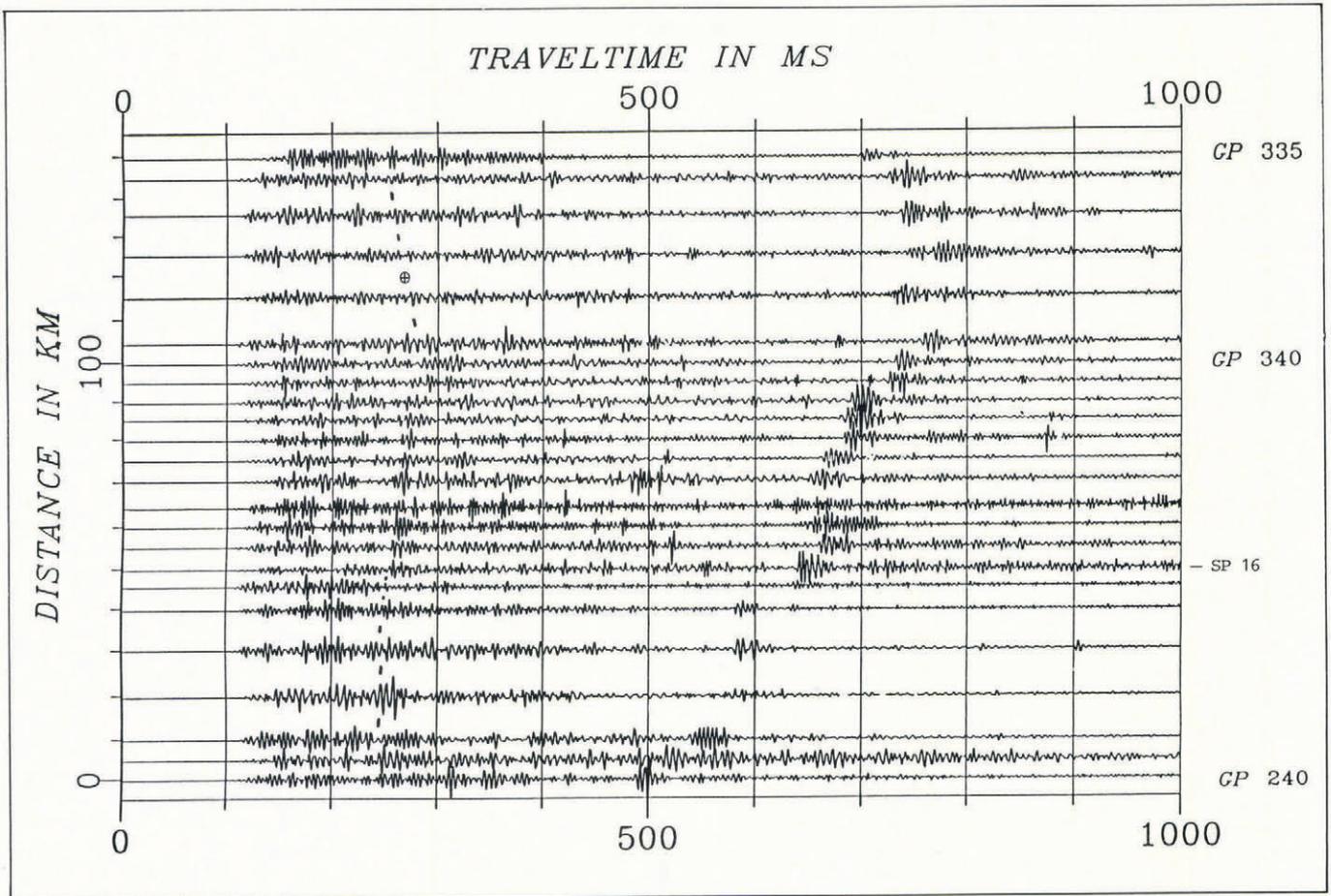

Fig. 4. A section of data after final processing, showing the distance of shot points with respect to grid point 240 versus travel time. Every trace is derived from the velocity analysis of a single record. The structure marked "- -" shows the trend of the ice-bottom reflection. In one case (symbol ⊕) the travel time is deduced from multiple reflections. The sea bottom appears at travel times greater than 500 ms. A return from the internal horizon is not visible.

TABLE I. ICE AND SEA-BOTTOM DATA REVEALED FROM REFLECTION-SEISMIC MEASUREMENTS (sea bottom at the ice front from Kohnen (1982))

| GP	Profile distance	Coordinates		Ice thickness	Water depth below sea-level
	km	W	S	m	m
ice front	−122			−	230
	−108			195	317
140	−102			220	344
240	0	52°48.25'	77°52.03'	422	547
	+ 5			426	572
	+ 10			430	592
	+ 20			433	609
	+ 30			439	624
	+ 40			444	631
	+ 45			444	668
241	+ 50	54°02.82'	78°14.51'	448	676
	+ 55			452	693
	+ 60			455	689
	+ 65			457	679
	+ 70			463	692
	+ 75			469	705
	+ 80			472	722
	+ 85			478	725
	+ 90			480	731
	+ 95			485	763
340	+100	55°25.9'	78°36.37'	493	771
	+105			504	797
	+115			486	764
	+120			486	768
	+125			477	770
	+135			459	756
	+145			450	740
335	+150	57°09.57'	78°19.25'	447	720
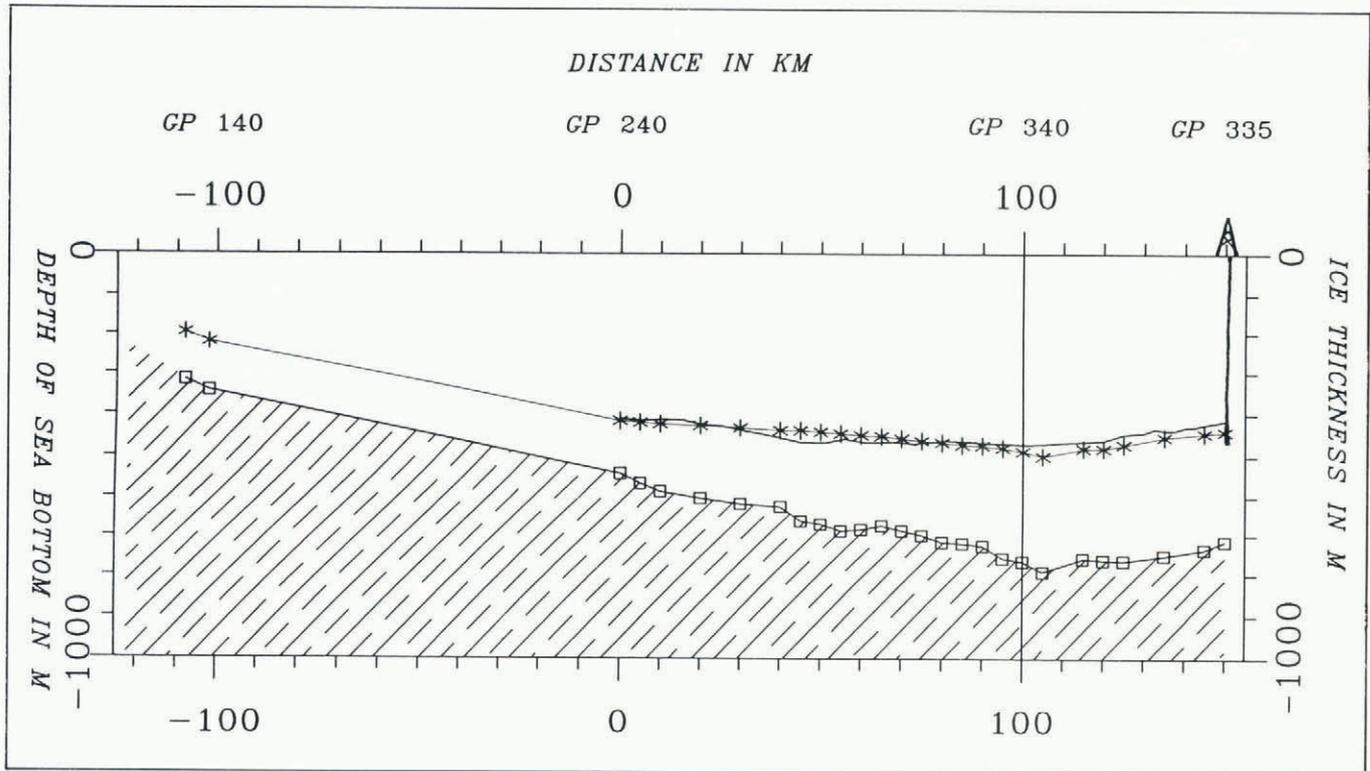
Fig. 5. Ice and sea-bottom profiles on a cross-section of Filchner–Ronne Ice Shelf extending inland from the ice front. Ice thicknesses from seismic measurements (medium line, stars), ice thicknesses from isostasy (heavy line) from Thyssen (1988, this volume), 465 m drill hole at grid point 335 from Engelhardt and Determann (1987).

the orientation of the line is supported by the travel time deduced from a multiple reflection recorded at profile km 120. When a correlation of the ice-bottom reflector is carried out, the extraction of travel times at shot point t_0 is possible. With t_0 and the ice thickness it is easy to obtain the amount of water beneath the ice shelf from the existing travel times of the sea-bottom reflector, taking a sea-water velocity of 1480 m/s. The final results are shown in Table I. Estimated errors include an uncertainty of ±5 ms for travel times and ±50 m/s for seismic velocities, giving overall errors of less than 20 m for depths of ice and the sea bottom.

DISCUSSION AND CONCLUSION

The ice depths revealed by seismic investigations can be compared with data from an aerogeophysical survey (Thyssen 1988, this volume) running parallel to the seismic profile and yielding altitudes of the ice surface. According to the buoyancy of the ice shelf, thicknesses can be derived from the height of the surface above sea-level, even if the uncertain density below the internal horizon causes some deviations. Errors in the measurement of seismic depths are almost equivalent to those obtained from considering hydrostatic equilibrium (Fig. 5).

The end of the seismic profile coincides with the location of a drill hole that reached the ice bottom at about 465 ± 5 m depth, in good agreement with the seismic value of 447 ± 20 m. Although seismic reflections from the sea bottom are easy to obtain, errors in sea depth are strongly affected by uncertainties in the ice thickness. Summing up, it may be concluded that seismic investigations can be successful in obtaining ice-bottom depths, even in places where electromagnetic techniques fail, provided that distances between shot points are sufficiently small. There are two more bands of thin ice in the west of FRIS, stretching back from the ice front to near the grounding line (Crabtree and Doake 1986; Thyssen 1988, this volume). It would be advisable to check these anomalies, which appear to be up to 300 m thinner than the surrounding areas, by more reflection-seismic measurements on a cross-profile.

REFERENCES

Crabtree, R.D., and C.S.M. Doake. 1986. Radio-echo investigations of Ronne Ice Shelf. *Ann. Glaciol.*, **8**, 37–41.

Engelhardt, H., and J. Determann. 1987. Borehole evidence for a thick layer of basal ice in the central Ronne Ice Shelf. *Nature*, **327**(6120), 318–319.

Garotta, D., and D. Michon. 1967. Continuous analysis of the velocity function and the move out corrections. *Geophys. Prospect.*, **15**, 584–597.

Herrod, L.D.B., and S.W. Garrett. 1986. Geophysical field-work on the Ronne Ice Shelf, Antarctica. *First Break*, **4**(1), 9–14.

Kohnen, H. 1982. Glaciological investigations in the frontal zone of the Filchner and Ronne ice shelves. *Ann. Glaciol.*, **3**, 160–165.

Robin, G. de Q., C.S.M. Doake, H. Kohnen, R.D. Crabtree, S.R. Jordan, and D. Möller. 1983. Regime of the Filchner-Ronne ice shelves, Antarctica. *Nature*, **302**(5909), 582–586.

Thyssen, F. 1985. First results from Polar-2-measurements on the Filchner and Ekström ice shelves. *In* Kohnen, H., comp. *Filchner-Ronne-Ice-Shelf-Programme. Report No. 2*. Bremerhaven, Alfred-Wegener-Institute for Polar Research, 131–132.

Thyssen, F. 1986. The central part of the Filchner/Ronne Ice Shelf. *In* Kohnen, H., comp. *Filchner-Ronne-Ice-Shelf-Programme. Report No. 3*. Bremerhaven, Alfred-Wegener-Institute for Polar and Marine Research, 81–83.

Thyssen, F. 1988. Special aspects of the central part of Filchner—Ronne Ice Shelf, Antarctica. *Ann. Glaciol.*, **11**, 173–179.